Biomolecules and Biomedicine
ISSN: 2831-0896 (Print) | ISSN: 2831-090X (Online)
Journal Impact Factor® (2024): 2.2
CiteScore® (2024): 5.2
www.biomolbiomed.com | blog.bjbms.org

RESEARCH ARTICLE

Ilinčić et al: Tubular function and PTH in early CKD

Tubular functional capacity and maladaptive parathyroid hormone response in early-stage chronic kidney disease

Branislava Ilinčić[1,2*], Radmila Žeravica[1,2], Romana Mijović[2], Esma R. Isenović[3], Dragan Burić[1,2], Dragana Žuvić[1,2], Velibor Čabarkapa[1,2]

[1]Department of Pathophysiology and Laboratory Medicine, Faculty of Medicine, University of Novi Sad, Novi Sad, Serbia;

[2]Center for Laboratory Diagnostic and Nuclear Medicine, University Clinical Centre of Vojvodina, Novi Sad, Serbia;

[3] Department of Radiobiology and Molecular Genetics, VINČA Institute of Nuclear Sciences-National Institute of the Republic of Serbia, University of Belgrade, Belgrade, Serbia.

*Correspondence to Branislava Ilinčić: branislava.ilincic@mf.uns.ac.rs

DOI: https://doi.org/10.17305/bb.2025.13395

ABSTRACT

Clinical data regarding the interaction between tubular functional capacity (TFC) and maladaptive parathyroid gland response in early-stage chronic kidney disease (CKD) are limited. This study aimed to evaluate the association between parathyroid gland response, measured as intact parathyroid hormone (iPTH) serum concentration (pg/mL) using chemiluminescent microparticle immunoassay, and the dissociation between the decline in glomerular filtration rate (GFR) and TFC, assessed through radionuclide clearances. TFC was evaluated by measuring effective renal plasma flow (mERPF, ml/min/1.73m²) using (131I) Hippurate (131I-H) clearance, while GFR was measured using (99m) Tc-DTPA (mGFR, ml/min/1.73m²). Consecutive participants with preexisting CKD (N=111, female 44%, male 56%) were enrolled and stratified into four groups based on CKD stages (1, 2, 3a, and 3b). Median serum iPTH concentrations significantly differed between Stage 1 [23 (20.4-25.5) pg/mL] and Stage 2 [23.6 (20.5-26.8) pg/mL] compared to Stage 3a [38.1 (34.1-41.9) pg/mL] and Stage 3b [45.8 (39.7-51.9) pg/mL] (p=0.01). In Stage 1, there was a significant positive association between iPTH and mERPF (p=0.003). Conversely, in Stage 3b, iPTH was significantly negatively associated with both mGFR and mERPF (p<0.05 for both). Regression models that included the interaction between CKD stage and either mGFR or mERPF, alongside other predictors (age, CKD stage, body mass index, ionized calcium, and 25-hydroxyvitamin D), revealed significant associations with iPTH (p<0.05 for all variables). The assessment of TFC using 131I-H plasma clearance does not enhance the detection of maladaptive parathyroid gland responses compared to evaluating CKD stage and its relationship with declining glomerular and tubular clearances in early-stage CKD patients.

Keywords: Tubular functional capacity, effective renal plasma flow, glomerular filtration rate, intact parathyroid hormone, chronic kidney failure.

INTRODUCTION

At present, hyperparathyroidism (HPT) is a relatively common condition, often detected through biochemical screening without any known preceding clinical signs of parathyroid gland disease. The various clinical profiles of HPT, including primary (asymptomatic, normocalcemic variants, hypercalcemic HPT), regulatory, secondary (SHPT), and tertiary (THPT), share a common feature of overactive parathyroid gland secretion and downregulation of the calcium-sensing receptor (CaSR). These shared characteristics result from a variety of etiological factors, including genetic and epigenetic alterations (1, 2). Alongside PHPT and THPT, which have a clear etiology (3-5), regulatory and SHPT are consequences of prolonged hyperphosphatemia and hypocalcaemia due to multiple metabolic and target organ dysfunctions, including renal, bone, gastrointestinal, neuro, and liver diseases (6).

The complexity of evaluating possible causes and consequences of chronic kidney disease (CKD), particularly in the elderly population, provides opportunities for a better understanding of increased maladaptive parathyroid hormone (PTH) secretion. It also broadens perspectives on the impact of SHPT on bone metabolism abnormalities, heterotopic vascular and soft tissue calcifications, cardiovascular events, and mortality (7). Regardless of the primary etiology of CKD, a decrease in glomerular filtration rate (GFR) has numerous consequences and is considered one of the most important causes of maladaptive parathyroid gland response in SHPT. Early-stage CKD, defined as stages 1 to 3, is often asymptomatic and frequently goes undiagnosed (8). Disruption of PTH secretion emerges in the early stages of CKD, in response to the interaction between calcium, phosphate, active vitamin D, and fibroblast growth factor 23 (FGF23) (9). After an initial decline in FGF23 and impaired inhibitory feedback mechanisms in the parathyroid glands, serum PTH concentrations begin to rise when the GFR falls below 60 mL/min/1.73 m^2 (10). Furthermore, impaired renal clearance of PTH, a process in which the kidneys and liver play a crucial role, contributes to SHPT in CKD (11). The research that investigated renal extraction of PTH has underscored the importance of peritubular clearance, a process through which most of PTH (1-84) and amino-terminal and carboxy-terminal PTH fragments are cleared from the circulation, bypassing GFR (12, 13). Given the theoretical possibility that renal tubular injury could precede glomerular injury, and the potential for a significant decrement in tubular function even in the presence of “normal” GFR, the characterization of tubular functional

capacity (TFC) could be a valuable tool in the evaluation of PTH levels in the early stages of CKD (14, 15).

The present study, with its meticulous design, aimed to explore the utility of characterizing the association between parathyroid gland response and the dissociation between the decline in glomerular filtration rate (GFR) and TFC, assessed by radionuclide clearances. Estimating TFC using effective renal plasma flow (ERPF), a key component of renal plasma blood flow that supplies the secretory active structures of the kidney, enhances the reliability and validity of the findings.

MATERIALS AND METHODS

Study subjects and protocol

An observational, cross-sectional study was done at the University Clinical Center of Vojvodina (UCCV). Consecutive participants were enrolled in the study and referred to the Department of Laboratory Diagnostic and Nuclear Medicine at UCCV for kidney function assessment using radionuclide renal clearances. Patients with previously diagnosed CKD due to chronic tubulointerstitial diseases were referred for evaluation of baseline kidney function to initiation of potentially nephrotoxic therapies. A standardised protocol for all patients who underwent radionuclide renal clearances included two visits. During the first visit of our department, radionuclide renal clearance for measurement of GRF (mGFR) and venous blood sampling for laboratory analysis were performed between 7 and 9 am, in a fasting state, 12 hours after the last meal. The second visit occurred within seven days of the first, provided there was no change in the patient's clinical status, and involved radionuclide renal clearance for the measurement of effective renal plasma flow (mERPF). Anthropometric measurements were taken at both visits, including body height (BH), body weight (BW), and waist circumference (WC). Body mass index (BMI = BW/BH^2, kg/m^2) and body surface area (BSA) were also calculated. Patients provided two urine samples: a 24-hour collection during the first visit and a first-morning sample during the second visit. If both results were classified within the same albuminuria category, the patient data were included in the subsequent analysis.

The study included both genders, female (49/111 - 44%) and male (62/111 -56%) participants. Patients were classified within GFR categories G1, G2, G3a, and G3b, and with kidney damage who exhibited albuminuria in categories A1 and A2 (16).

Patient were stratified into 4 groups: Stage 1 (mGFR ≥90 ml/min/1.73m^2 with kidney damage, N= 25), Stage 2 (mGFR 60–89 ml/min/1.73m^2 with kidney damage, N= 30), Stage 3a (mGFR 45–59 ml/min/1.73m^2, N= 26), Stage 3b (mGFR 30–44 ml/min/1.73m^2, N= 30). Patients with albuminuria category A3 (AER>300 mg/24 h) were excluded from further testing due to methodological constraints and the risk of overestimating expanded body space in cases of severe albuminuria. Also, the study excluded patients with CKD stage 4 and 5, diabetes mellitus, liver and gastrointestinal diseases, inflammatory, autoimmune and infectious diseases, endocrine gland dysfunctionalities, malignancies, subjects exhibiting clinically evident oedema or ascites, pregnancy, and medications taken routinely that could affect PTH level [corticosteroids, estrogen replacement, biotin supplementation, diuretics, sodium-glucose contransporter-2 inhibitors, lithium, anticonvulsants (phenytoin/phenobarbital), bisphosphonates, denosumab, romosozumab, calcitonin, calcium channel blockers).

Radionuclide renal clearance

Radionuclide renal clearance methods were performed according to established standard operating procedures (17, 18) and local protocols. Following hydration with water (5 mL water/kg body mass), plasma clearances were obtained using a single injection of a commercially available radiopharmaceutical. A blood sampling schedule was specified for GFR after 180 and 240 minutes following the intravenous injection of 30 MBq technetium (99mTc) pentetate (DTPA) - (99m)Tc-DTPA (Technescan DTPA, Mallinckrodt Medical B.V., Netherlands). For ERPF, after 20 and 30 minutes from intravenous application of 1 MBq Hippurate (131I-H) (Institute for Nuclear Science, Vinca, Serbia). Venous blood samples were collected from the contralateral limb to reduce the risk of contamination. The radioactivity of plasma samples was measured using a well gamma counter with a NaI(Tl) crystal (Captus 3000 by Capintec, USA) with appropriate energy windows for (99m)Tc and (131)I. Daily quality control was performed in accordance with the manufacturer's recommendations. Calculations for mGFR and mERPF were done according to the slope-intercept method [Captus 3000 Builtin Software, version 1.28 (2013)]. The Brochner-Mortensen correction was used for mGFR calculation, and mERPF was adjusted by multiplying by 0.8 (to account for a 20% overestimation of ERPF)(19). Obtained values were normalized to individually calculated BSA employing the

DuBois and DuBois formula (20). Corrected mGFR and mERPF values were compared to age- and sex-specific reference values (ASS GFR and ASS ERPF) (21), and the absolute and relative deviation for age and sex specific GFR (DEV ASS GFR, ml/min/1.73m^2, %) and absolute and relative deviation for age and sex specific ERPF (DEV ASS ERPF, ml/min/1.73m^2, %) were calculated.

ASS GFR = 144.1 - (0.99 × age) female; ASS GFR = 160.5 - (1.16 × age) male

ASS ERPF= 673,3 – (2,92 x age) female; ASE-ERPF: 854,2-(5,4 x age) male

Chromatography was performed for quality control of the radiochemical purity (RCP): paper chromatography for (99m) Tc-DTPA RCP >95%; thin layer chromatography for Hippurate – (131) I; (Hippuric – (131)I) ≥96%; radiochemical impurity: % (131)I≤2% and 2-iodo(131I) benzoic acid ≤2%.

Biochemical analyses

Serum concentrations of glucose, urea, creatinine, uric acid, total calcium (t Ca), ionized calcium (i Ca), phosphorus (P), and magnesium (Mg) were measured using spectrophotometric methods on an automated analyzer (Alinity c, Abbott). Serum ionized calcium (iCa) was measured using an ion-selective electrode method on the AVL 9180 analyzer (Roche Diagnostics). Lipid profile parameters, including total cholesterol (t Chol), triglycerides (TG), and high-density lipoprotein cholesterol (HDL-C), were determined spectrophotometrically using the Alinity c analyzer. Low-density lipoprotein cholesterol (LDL-C) was calculated using Friedewald's formula. Apolipoproteins Apo AI and Apo B were quantified by immunoturbidimetric assay. Serum cystatin C concentrations were measured by the nephelometric method on the BN ProSpec System (Siemens). Albuminuria excretion rate (AER, mg/24 h) was assessed in 24-hour urine samples using an immunoturbidimetric method on the Alinity c analyzer. In a spot urine sample, albumin and creatinine concentrations were measured, and the albumin-to-creatinine ratio (ACR, mg/mmol) was calculated.

Serum concentrations of insulin, 25-hydroxyvitamin D [25(OH)D], and intact parathyroid hormone (iPTH) were determined using chemiluminescent microparticle immunoassay (CMIA) on the Alinity i analyzer (Abbott). Vitamin D deficiency was defined as serum 25(OH)D levels below 50 nmol/L (22). The insulin resistance index (Homeostasis Model Assessment – Insulin Resistance, HOMA-IR) was calculated for all participants (23). The RR for iPTH in adults was 15–68.3 pg/mL. Internal

laboratory quality control was performed to assess the measurement of iPTH serum concentration. iPTH levels were monitored over 20 days, using control levels provided by three manufacturers (low, medium, and high control; iPTH STAT Protocol, Abbott) and two different iPTH concentrations in blood samples (pool serum). Imprecision (CV total) and BIAS (apsolute and relative) were consistent with the manufacturer's specification: low control 8.3 pg/mL (CV 4.4%, BIAS:0,67; BIAS%- 8.08%); medium control 54.2 pg/mL (CV 3,9%; BIAS:1,85; BIAS%- 3.41%); high control 208.3 pg/mL (CV 4.0%, BIAS: 7,75; BIAS%- 3.72%); I pool - 74.8 pg/mL (CV 3.2%, BIAS:- -8.40; BIAS%: 11.23%) and II pool 156.2 pg/mL (CV: 4.2%, BIAS: - 22,56; BIAS%:14.44%).

Ethical statement

The study was conducted according to the guidelines of the Declaration of Helsinki and approved by the Ethics Committee of UCCV (No.00-347/2025). All participants provided written informed consent before participating in the study. All methods were carried out in accordance with relevant guidelines and regulations.

Statistical analysis

The distribution of the variables was determined using the Shapiro-Wilk test. Continuous variables with normal distribution are presented as mean ± standard deviation, while non-normally distributed variables are shown as median and values of the lower and upper quartiles (Q1-Q3). Depending on the data distribution, ANOVA or the Kruskal-Wallis test was used for multiple-group comparisons, with a Bonferroni post hoc multiple comparison. Spearman's rank correlation coefficient was used to describe monotone relationships between iPTH serum concentration and other continuous variables. Scatter plots were used to visualize relationships between iPTH and the independent variables (renal clearance measurements: mGFR and mERPF) in the study group. Univariate linear regression analyses were first performed separately for each stage 1-3b group to explore the relationships between iPTH and renal clearances. Multivariate linear regression models with interactions were used to examine the relationship between iPTH and variables associated with kidney profile. The variables included renal clearance measurements, CKD stage, interactions between CKD stage and mGFR, and mERPF. To prevent confounding between

mGFR and mERPF, each variable was analyzed in a separate model (GFR model and ERPF model). Subsequently, multivariate linear regression models were used to evaluate predictors of iPTH serum concentration. Cys C and P serum concentrations were excluded as they showed no significant effect in initial model analyses. Model 1 included CKD stage, interaction (CKD stage x mGFR), age, BMI, iCa and 25(OH)D; model 2 included CKD stage, interaction (CKD stage x mERPF), age, BMI, iCa and 25(OH)D. Residuals were analyzed for both models, and collinearity was assessed using tolerance. Models were compared using Akaike's information criterion (AIC). Statistical significance was set at an alpha level of 0.05. Analyses were conducted using statistical software Stata 18, StataCorp LLC 2023, and statistical software Statistica 14.0.0.15, TIBCO Software Inc.

RESULTS

Table 1 presents a comparison of clinical, metabolic, and mineral profiles across patient groups. Patients in Stage 3a and 3b had significantly higher median ages than those in Stages 1 and 2 ($P < 0.001$). No statistically significant differences were observed in anthropometric measurements (BMI and WC) or blood pressure values (SP, DP, MAP) between the groups. Analysis of laboratory parameters revealed that median levels of glucose and lipids, including HDL-C, TG, and apo AI, differed significantly between groups (all $P < 0.05$). In contrast, no significant differences were found in the median serum concentrations of electrolytes (iCa, P, Mg) or 25(OH)D. Among all patients, 47% exhibited concomitant vitamin D deficiency. The median serum concentrations of iPTH in the Stage 1 and Stage 2 groups [23 (20.4-25.5) vs. 23.6 (20.5-26.8) pg/mL, $P>0.05$] were significantly lower ($P=0.01$) than those in the Stage 3a and Stage 3b groups [38.1 (34.1-41.9) vs. 45.8 (39.7-51.9) pg/mL, $P>0.05$]. Renal function profile parameters demonstrated consistent statistical significance across groups (Table 2). Median cys C serum concentrations did not differ significantly between Stage 1 and Stage 2, but were significantly lower in Stages 1 and 2 compared to Stages 3a and 3b. Both mGFR and mERPF values declined significantly with each advancing stage ($P<0.05$ for both). DEV ASS GFR (%) and DEV ASS ERPF (%) demonstrated statistically significant differences across all stages ($P<0.05$ for both).

Spearman correlation analysis (Table 3) revealed statistically significant positive monotone relationships between iPTH and age ($r = 0.42$, $P < 0.01$), WC ($r = 0.22$, $P = 0.02$), BMI ($r = 0.27$, $P = 0.01$), and cys C ($r = 0.48$, $P < 0.01$). Statistically significant negative monotone relationships were observed between iPTH and 25(OH)D ($r = -0.19$, $P=0.04$), mGFR ($r = -0.66$, $P < 0.01$), and mERPF ($r = -0.68$, $P < 0.01$).

In all patients (N=111), a scatter plot with fitted regression lines and 95% confidence intervals shows a linear relationship between iPTH and mERPF (Figure 1), with the regression equation iPTH = 60.67 - 0.08*mERPF. Figure 2 illustrates a linear relationship between iPTH and mGFR, with the regression equation iPTH=59.75 - 0.41*mGFR.

Table 4 displays the univariate linear regression results examining the relationship between serum iPTH concentration and renal clearance measurements (mGFR and mERPF) across stages 1 to 3b. Group analyses revealed a significant negative linear association between mGFR and iPTH in stage 3b ($P=0.007$). Also, in CKD stage 3b, a significant negative linear association between mERPF and iPTH was observed ($P=0.001$). In stage 1, mERPF and iPTH showed a significant positive association ($P=0.003$).

Table 5 summarizes the relationship between serum iPTH concentration and variables associated with kidney profile. In the GFR model ($R^2 = 0.68$, adjusted $R^2 = 0.46$, $P < 0.001$), both variables CKD stage ($\beta = 0.922$, $P = 0.01$) and the interaction (CKD stage x mGFR) ($\beta = - 0.297$, $P = 0.006$) were significantly associated with serum iPTH concentration. In the ERPF model ($R^2 = 0.72$, adjusted $R^2 = 0.52$, $P < 0.001$), CKD stage ($\beta = 1.423$, $P < 0.001$) and interaction (CKD stage x mERPF) ($\beta = -0.605$, $P < 0.001$) were also significantly associated with serum iPTH concentration.

The results of the multivariate regression models are presented in Table 6. In model 1 ($R^2 = 0.79$, adjusted $R^2 = 0.63$, $P < 0.001$; AIC = 814.645), CKD stage ($\beta = 0.978$, $P < 0.001$), (CKD stage x mGFR) interaction ($\beta = -0.347$, $P < 0.001$), age ($\beta = -0.157$, < 0.001), BMI ($\beta = 0.202$, $P < 0.001$), iCa ($\beta = -0.228$, $P < 0.001$), and 25(OH)D ($\beta = -0.325$, $P <0.001$) were each independently and significantly associated with serum iPTH concentration. In this model, each increase in CKD stage was associated with a 12.85 pg/mL increase in iPTH serum concentration.

In model 2 ($R^2 = 0.80$, adjusted $R^2 = 0.65$, $P < 0.001$; AIC = 807.216), CKD stage($\beta = 1.007$, $P < 0.001$), (CKD stage x mERPF) interaction ($\beta = -0.398$, $P < 0.001$), age ($\beta = -0.169$, < 0.001), BMI ($\beta = 0.203$, $P = 0.001$), iCa ($\beta = - 0.158$, $P = 0.009$), and 25(OH)D ($\beta = -0.323$, $P < 0.001$) were each independently and significantly associated with serum iPTH concentration. In model 2, each increase in CKD stage was associated with a 13.23 pg/mL increase in iPTH serum concentration.

Table 6

DISCUSSION

This study evaluates indicators of glomerular function and TFC by radionuclide clearances in patients with CKD, and their relation to iPTH levels across early stages. The novelty of this study lay in the observation of TFC through the measurement of ERPF, as part of the renal plasma flow that irrigates the secretory active structures of the kidney (24, 25).

In summary, this study found a significant negative correlation between mGFR, mERPF, and iPTH in early-stage CKD. When analyzing CKD stages separately, there was a significant negative linear association between iPTH and both mGFR and mERPF in stage 3b (GFR 30–44 mL/min/1.73 m²). In stage 1 (mGFR ≥ 90 ml/min/1.73 m² with A1 or A2 categories), iPTH showed significant positive associations with mERPF. These findings underscore the role of tubular secretory pathways in regulating iPTH level. In addition to measured clearances for glomerular and tubular function, when examining the relationship between iPTH levels and overall kidney indicators, we found that TFC, measured by 131I-H plasma clearance, was not a significant predictor of iPTH levels in patients with early-stage CKD. In this expanded analysis, we found a significant association between serum iPTH concentration and the interaction between CKD stage and TFC. Similarly, in the model focusing on glomerular function, CKD stage and the interaction between CKD stage and GFR was independently and significantly associated with iPTH level.

The prevalence of SHPT in patients with CKD remains high, regardless of diagnostic criteria. A recent study by Wang and authors reported a prevalence of 49.5%. (26). Most measured iPTH levels in our study were within the reference range (15–68.3 pg/mL). Median iPTH levels did not differ significantly between Stage 1 and Stage 2, but levels in Stages 1 and 2 were significantly lower than in Stages 3a and 3b. Also,

our results showed that each increase in CKD stage was associated with a 13 pg/mL increase in iPTH level, regardless of whether the predictor was the interaction between CKD stage and GFR or TFC. The present findings are consistent with previous studies (7, 27), indicating a potential increase in iPTH levels as GFR decreases to below 60 mL/min/1.73 m². Current guidelines recommend monitoring iPTH levels in patients with stage 3 chronic kidney disease (CKD) when GFR falls below this threshold. Notably, the guidelines also state that the optimal PTH level for stage 3 CKD patients remains undetermined, as does the reference range adjusted for age and 25(OH) vitamin D levels in this vulnerable population (16).

Further, mERPF showed statistically significant negative linear coefficients to iPTH level in CKD stage 3b. There is a lack of published studies about the association between ERPF as a possible indicator of TFC and iPTH level. Clinical evaluation of tubular secretion as an early, independent marker is limited by a lack of precise quantification methods, variable patient hydration, concurrent drug therapies, and the complexity of timed urine collections with changing flow rates (25). Physiologically, tubular secretion is the primary renal mechanism for eliminating most drugs and their metabolites, and it should be routinely measured. In humans, 131I-H is about 15% lower than para-aminohippuric acid (PAH) clearance, which is the gold standard for measuring ERPF (19, 28, 29).

According to the study of Fine and authors (19), the correlation with ERPF from PAH clearances is very high ($r = 0.90$, $p < 0.01$). PAH was not implemented in clinical practice because the analysis procedure was excessively complex. (30). The pharmacokinetic characteristics of 131I-H closely resemble those observed in PAH. Following intravenous administration, the bolus rapidly enters the renal circulation and reaches individual nephrons, where it is eliminated through both glomerular filtration (approximately 20%) and active tubular secretion (approximately 80%). Consequently, the excretion of 131I-H is directly proportional to the filtered plasma fraction. 131I-H passes into Bowman's space as primary urine, while the remaining plasma (four-fifths) exits the glomeruli via efferent arterioles and enters the peritubular capillaries. Proximal tubule cells then actively uptake, transport, and secrete the residual 131I-H into the urine through energy-dependent mechanisms. As a result, nearly the entire quantity of 131I-H present in each blood volume is removed and excreted in the urine during a single renal passage (29, 31). A small fraction of

renal blood flow, slightly exceeding 10%, supplies the medullary structures, the hilus, and the capsule of the kidney. These regions lack a transport system for the extraction of organic anions, including 131I-H. Goldring et al. introduced the term ERPF to describe the portion of renal plasma flow that supplies the kidney's secretory active structures (28). According to different authors, the extraction efficiency of the kidneys for 131I-H ranges from 0.84-0.94 (29). In addition to 131I-H, 99mTc-ethylene dicysteine (99mTc-EC) is an important agent for estimating renal tubular function. In both healthy individuals and patients, the plasma clearance of 99mTc-EC closely correlates with the clearance of 131I-H and is approximately 75% of the 131I-H values. The renal extraction ratio for 99mTc-EC is 0.70 (32).

Various etiologies of CKD could differently affect the dissociation between the decline in GFR and TFC. Therefore, a widely available evaluation of GFR is insufficient to get deeper insight into early abnormalities. Tubular dysfunction frequently remains under-recognized and under-diagnosed at earlier stages of CKD. In this study, ASS ERPF and ASS GFR values further enable precision in result interpretation. Monitoring tubular function, in addition to GFR, in patients prone to SHPT, elderly, and vitamin D-deficient patients with CKD-related diseases (i.e., hypertension, diabetes) could delay the development of SHPT and prevent resistance to dietary/dialytic/pharmacological therapy. These findings suggest that a comprehensive approach to CKD management, which includes monitoring of TFC, could be beneficial.

In our study, iCa level was a significant negative predictor of iPTH level. Patients showed no abnormal changes in mineral profiles, including serum phosphate retention or hypocalcemia. These electrolyte imbalances are the primary factors leading to SHPT, characterized by a GRF below 60 ml/min per 1.73 m². Impairment of renal clearance of PTH in early CKD stages due to a decrease of TFC (renal peritubular uptake is the dominant mechanism of PTH 1–84 clearance from the circulation by the kidney), evaluated with mERPF in this study, could be one of the possible mechanisms that leads to shifting iPTH level towards higher values (33). Also, in addition to significant age-related functional declining changes in target organs (kidney, bone, intestine) and dysregulation of mineral homeostasis for the development of SHPT (34), results from our study confirm previous findings that a decrease in mGFR and mERPF, we observed a corresponding significant increase in iPTH serum concentrations in CKD stage 1-3b patients. Evidence from studies shows

that maintaining the levels of phosphate and PTH within normal ranges is important for the prevention of further kidney function deterioration and CV incidence (9). The multifactorial vulnerability of CKD patients with SHPT may increase CVD mortality and morbidity by contributing to vascular calcification and promoting PTH1R expression in the cardiovascular system. (35). Our study shows that these patients have increased levels of proatherogenic lipid particles, lower HDL-C, and higher TG levels as CKD stage advances.

We observed a statistically significant association between iPTH level and biological determinants, such as age, BMI, and 25 (OH)D level. Earlier studies revealed biological factors influencing PTH level, in addition to age, sex, and lifestyle factors (consumption of plant foods), genetics (variants located near genes involved in vitamin D metabolism, and Ca and renal P transport) account for 60% of variations in PTH levels (36, 37). In our study, age and 25(OH)D level were independently and significantly associated with the iPTH level in CKD patients, in concordance with similar studies (37), highlighting the importance of these factors in interpreting the results. Pulsatile fluctuations and circadian rhythms influence variations in circulating PTH levels. These physiological changes may impact the accuracy of measured circulating PTH concentrations. To address variability in iPTH levels caused by intrinsic and extrinsic factors (38, 39), we analyze laboratory parameters, monitor quality control, and assess biological activity in vivo. Due to the limited availability of EDTA plasma, iPTH was measured in serum samples. Serum may yield slightly lower iPTH concentrations than EDTA plasma because peptide degradation during clotting can introduce matrix-related bias.

The study is limited by a relatively small patient cohort, a restricted range of CKD etiologies focused on chronic tubulointerstitial diseases, and reduced sample size due to time constraints. Additionally, incorporating measurements of other urinary biomarkers of renal tubular damage, such as kidney injury molecule-1 (KIM-1) and N-acetyl-ß-glucosaminidase (NAG)(40), may enhance the specificity of the observed association between TFC and iPTH levels. While radionuclide plasma clearance is employed in this study to measure GFR and ERPF, all clearance methods are susceptible to systematic and random errors. Such errors may result in discrepancies between measured GFR and ERPF and the actual renal function. Additionally, biological conditions and analytical factors can fluctuate over time, contributing to variability in the measured parameters (40). Notably, this study is the first to

demonstrate a relationship between intact parathyroid hormone (iPTH) levels and measured ERPF (mERPF) in patients with early-stage chronic kidney disease (CKD). Future investigations should assess both clearances concurrently, preferably utilizing clinically available, non-radioactive substances.

CONCLUSION

Results from this study suggest that assessing TFC decline using 131I-H plasma clearance may help identify the decline in TFC in patients with early-stage CKD. However, assessing TFC with 131I-H plasma clearance does not improve the detection of maladaptive parathyroid gland responses compared to evaluating CKD stage and its association with declining glomerular and tubular clearances in early-stage CKD patients.

ACKNOWLEDGMENTS

This work was partially supported by the Ministry of Science, Technological Development, and Innovation of the Republic of Serbia (Contract No# 451-03-136/2025-03/ 200017).

Conflicts of interest: Authors declare no conflicts of interest.

Funding: Authors received no specific funding for this work.

Data availability: The data associated with the manuscript are available from the corresponding author upon reasonable request.

Submitted: October 18, 2025

Accepted: December 23, 2025

Published online: December 26, 2025

REFERENCES

1. Deluque AL, Dimke H, Alexander RT. Biology of calcium homeostasis regulation in intestine and kidney. Nephrol Dial Transplant. 2025;40(3):435–45. https://doi.org/10.1093/ndt/gfae204

2. Li X, Lu Y, Zhang L, Song A, Zhang H, Pang B, et al. Primary and secondary hyperparathyroidism present different expressions of calcium-sensing receptor. BMC Surg. 2023;23(1):31. https://doi.org/10.1186/s12893-023-01928-5

3. Palumbo VD, Palumbo VD, Damiano G, Messina M, Fazzotta S, Lo Monte G, et al. Tertiary hyperparathyroidism: a review. Clin Ter. 2021;172(3):241–6.

4. Singh P, Bhadada SK, Dahiya D, Arya AK, Saikia UN, Sachdeva N, et al. Reduced Calcium Sensing Receptor (CaSR) Expression Is Epigenetically Deregulated in Parathyroid Adenomas. J Clin Endocrinol Metab. 2020;105(9):3015–24. https://doi.org/10.1210/clinem/dgaa419

5. Arya AK, Kumari P, Singh P, Bhadada SK. Molecular basis of symptomatic sporadic primary hyperparathyroidism: New frontiers in pathogenesis. Best Pract Res Clin Endocrinol Metab. 2025;39(2):101985. https://doi.org/10.1016/j.beem.2025.101985

6. Lemoine S, Figueres L, Bacchetta J, Frey S, Dubourg L. Calcium homeostasis and hyperparathyroidism: Nephrologic and endocrinologic points of view. Ann Endocrinol (Paris). 2022;83(4):237–43. https://doi.org/10.1016/j.ando.2022.05.003

7. Tsai SH, Kan WC, Jhen RN, Chang YM, Kao JL, Lai HY, et al. Secondary hyperparathyroidism in chronic kidney disease: A narrative review focus on therapeutic strategy. Clin Med (Lond). 2024;24(5):100238. https://doi.org/10.1016/j.clinme.2024.100238

8. Kushner P, Khunti K, Cebrián A, Deed G. Early Identification and Management of Chronic Kidney Disease: A Narrative Review of the Crucial Role of Primary Care

Practitioners. Adv Ther. 2024;41(10):3757–70.
https://doi.org/10.1007/s12325-024-02957-z

9. Bozic M, Diaz-Tocados JM, Bermudez-Lopez M, Forné C, Martinez C, Fernandez E, et al. Independent effects of secondary hyperparathyroidism and hyperphosphataemia on chronic kidney disease progression and cardiovascular events: an analysis from the NEFRONA cohort. Nephrol Dial Transplant. 2022;37(4):663–72.
https://doi.org/10.1093/ndt/gfab184

10. Khundmiri SJ, Murray RD, Lederer E. PTH and Vitamin D. Compr Physiol. 2016;6(2):561–601.
https://doi.org/10.1002/j.2040-4603.2016.tb00690.x

11. Ulmer CZ, Kritmetapak K, Singh RJ, Vesper HW, Kumar R. High-Resolution Mass Spectrometry for the Measurement of PTH and PTH Fragments: Insights into PTH Physiology and Bioactivity. J Am Soc Nephrol. 2022;33(8):1448–58.
https://doi.org/10.1681/ASN.2022010036

12. Muntner P, Jones TM, Hyre AD, Melamed ML, Alper A, Raggi P, et al. Association of serum intact parathyroid hormone with lower estimated glomerular filtration rate. Clin J Am Soc Nephrol. 2009;4(1):186–94.
https://doi.org/10.2215/CJN.03050608

13. van Ballegooijen AJ, Rhee EP, Elmariah S, de Boer IH, Kestenbaum B. Renal Clearance of Mineral Metabolism Biomarkers. J Am Soc Nephrol. 2016;27(2):392–7.
https://doi.org/10.1681/ASN.2014121253

14. Martin K, Hruska K, Greenwalt A, Klahr S, Slatopolsky E. Selective uptake of intact parathyroid hormone by the liver: differences between hepatic and renal uptake. J Clin Invest. 1976;58(4):781–8.
https://doi.org/10.1172/JCI108529

15. Dowling TC, Frye RF, Fraley DS, Matzke GR. Characterization of tubular functional capacity in humans using para-aminohippurate and famotidine. Kidney Int. 2001;59(1):295–303.
https://doi.org/10.1046/j.1523-1755.2001.00491.x

16. KDIGO 2024 Clinical Practice Guideline for the Evaluation and Management of Chronic Kidney Disease. Kidney Int. 2024;105(4 Suppl):S117–S314. https://doi.org/10.1016/j.kint.2023.10.018

17. Fleming JS, Zivanovic MA, Blake GM, Burniston M, Cosgriff PS. Guidelines for the measurement of glomerular filtration rate using plasma sampling. Nucl Med Commun. 2004;25(8):759–69. https://doi.org/10.1097/01.mnm.0000136715.71820.4a

18. Blaufox MD, Merrill JP. Simplified hippuran clearance. Measurement of renal function in man with simplified hippuran clearances. Nephron. 1966;3(5):274–81. https://doi.org/10.1159/000179542

19. Fine EJ, Axelrod M, Gorkin J, Saleemi K, Blaufox MD. Measurement of effective renal plasma flow: a comparison of methods. J Nucl Med. 1987;28(9):1393–400.

20. Du Bois D, Du Bois EF. A formula to estimate the approximate surface area if height and weight be known. 1916. Nutrition. 1989;5(5):303–11; discussion 12–3.

21. Schernthaner G, Erd W, Ludwig H, Sinzinger H, Höfer R. [Study of age and sex dependance in renal clearances with radioisotopes (author's transl)]. Aktuelle Gerontol. 1976;6(3):139–45.

22. Holick MF, Binkley NC, Bischoff-Ferrari HA, Gordon CM, Hanley DA, Heaney RP, et al. Evaluation, Treatment, and Prevention of Vitamin D Deficiency: an Endocrine Society Clinical Practice Guideline. The Journal of Clinical Endocrinology & Metabolism. 2011;96(7):1911–30. https://doi.org/10.1210/jc.2011-0385

23. Matthews DR, Hosker JP, Rudenski AS, Naylor BA, Treacher DF, Turner RC. Homeostasis model assessment: insulin resistance and beta-cell function from fasting plasma glucose and insulin concentrations in man. Diabetologia. 1985;28(7):412–9. https://doi.org/10.1007/BF00280883

24. Seegmiller JC, Wolfe BJ, Albtoush N, Melena I, Gross SP, Vinovskis C, et al. Tubular Secretion Markers, Glomerular Filtration Rate, Effective Renal Plasma Flow,

and Filtration Fraction in Healthy Adolescents. Kidney Med. 2020;2(5):670–2. https://doi.org/10.1016/j.xkme.2020.05.013

25. Alhummiany B, Sharma K, Buckley DL, Soe KK, Sourbron SP. Physiological confounders of renal blood flow measurement. Magma. 2024;37(4):565–82. https://doi.org/10.1007/s10334-023-01126-7

26. Wang Y, Liu J, Fang Y, Zhou S, Liu X, Li Z. Estimating the global prevalence of secondary hyperparathyroidism in patients with chronic kidney disease. Front Endocrinol (Lausanne). 2024;15:1400891. https://doi.org/10.3389/fendo.2024.1400891

27. Daimon M, Fujita T, Murabayashi M, Mizushiri S, Murakami H, Nishiya Y, et al. Exacerbation of Hyperparathyroidism, Secondary to a Reduction in Kidney Function, in Individuals With Vitamin D Deficiency. Frontiers in Medicine. 2020;7:221. https://doi.org/10.3389/fmed.2020.00221

28. Smith HW, Goldring W, Chasis H. THE MEASUREMENT OF THE TUBULAR EXCRETORY MASS, EFFECTIVE BLOOD FLOW AND FILTRATION RATE IN THE NORMAL HUMAN KIDNEY. J Clin Invest. 1938;17(3):263–78. https://doi.org/10.1172/JCI100950

29. Smith HW, Finkelstein N, Aliminosa L, Crawford B, Graber M. THE RENAL CLEARANCES OF SUBSTITUTED HIPPURIC ACID DERIVATIVES AND OTHER AROMATIC ACIDS IN DOG AND MAN. J Clin Invest. 1945;24(3):388–404. https://doi.org/10.1172/JCI101618

30. Durand E, Chaumet-Riffaud P, Grenier N. Functional renal imaging: new trends in radiology and nuclear medicine. Semin Nucl Med. 2011;41(1):61–72. https://doi.org/10.1053/j.semnuclmed.2010.08.003

31. Kumar R, Adiga A, Novack J, Etinger A, Chinitz L, Slater J, et al. The renal transport of hippurate and protein-bound solutes. Physiol Rep. 2020;8(4):e14349. https://doi.org/10.14814/phy2.14349

32. Kabasakal L. Technetium-99m ethylene dicysteine: a new renal tubular function agent. European Journal of Nuclear Medicine. 2000;27(3):351–7.
https://doi.org/10.1007/s002590050045

33. Kritmetapak K, Pongchaiyakul C. Parathyroid Hormone Measurement in Chronic Kidney Disease: From Basics to Clinical Implications. Int J Nephrol. 2019;2019:5496710.
https://doi.org/10.1155/2019/5496710

34. Irsik DL, Bollag WB, Isales CM. Renal Contributions to Age-Related Changes in Mineral Metabolism. JBMR Plus. 2021;5(10):e10517.
https://doi.org/10.1002/jbm4.10517

35. Towler DA. Parathyroid hormone-PTH1R signaling in cardiovascular disease and homeostasis. Trends Endocrinol Metab. 2024;35(7):648–60.
https://doi.org/10.1016/j.tem.2024.02.005

36. Robinson-Cohen C, Lutsey PL, Kleber ME, Nielson CM, Mitchell BD, Bis JC, et al. Genetic Variants Associated with Circulating Parathyroid Hormone. J Am Soc Nephrol. 2017;28(5):1553–65.
https://doi.org/10.1681/ASN.2016010069

37. Aloia JF, Feuerman M, Yeh JK. Reference range for serum parathyroid hormone. Endocr Pract. 2006;12(2):137–44.
https://doi.org/10.4158/EP.12.2.137

38. Yalla N, Bobba G, Guo G, Stankiewicz A, Ostlund R. Parathyroid hormone reference ranges in healthy individuals classified by vitamin D status. J Endocrinol Invest. 2019;42(11):1353–60.
https://doi.org/10.1007/s40618-019-01075-w

39. Smit MA, van Kinschot CMJ, van der Linden J, van Noord C, Kos S. Clinical Guidelines and PTH Measurement: Does Assay Generation Matter? Endocr Rev. 2019;40(6):1468–80.
https://doi.org/10.1210/er.2018-00220

40. McDonnell T, Söderberg M, Taal MW, Vuilleumier N, Kalra PA, group obotN-Cas. Plasma and Urinary KIM-1 in Chronic Kidney Disease: Prognostic Value, Associations with Albuminuria, and Implications for Kidney Failure and Mortality. American Journal of Nephrology. 2025.
https://doi.org/10.1159/000547867

TABLES AND FIGURES WITH LEGENDS

Table 1. Clinical, metabolic, and mineral profiles of patients

Variables	Stage 1 *n*=25	Stage 2 *n*=30	Stage 3a *n*=26	Stage 3b *n*=30	*p*
Age (years)	41[a] (18-66)	48[a] (22-70)	65[b] (43-82)	65[b] (22-77)	0.00
Male, N/total	16/25	16/30	10/26	20/30	0.14
BMI (kg/m^2)	27.4 ± 3.5	26.8 ±5.1	27.6 ±3.8	28.9 ± 4.2	0.29
WC (cm)	97.5 ±11.9	91.2 ±14.7	95.7 ±11.2	99.1 ±12.2	0.12
SP (mm Hg)	125.8 ±13.4	130.2 ±22.9	118.5 ±29.3	139.6 ±19.7	0.66
DP (mm Hg)	79.4 ±7.9	80.8 ±12.1	80.4 ±7.4	81.1 ±9.8	0.87
MAP (mm Hg)	94.8 ±8.8	97.3 ±15.5	94.9 ±12.6	97.3 ±12.3	0.72
Glucose (mmol/L)	5.3[a] (4.6-5.5)	5.01[a] (4.7-5.4)	5.4 [a,b] (4.98-6.1)	5.6[b] (5.3-6.1)	0.01
Insulin (mIU/L)	19 (9.7-25)	11.8 (8.2-15.5)	11.7 (7.8-17.8)	14.4 (11-32.3)	0.12
HOMA-IR	4.5 (2.2-6.2)	2.85 (1.8-3.7)	2.65 (1.7-4.9)	3.2 (2.4-7.8)	0.09
tChol (mmol/L)	5.4 (3.9-5.8)	5.2 (4.5-6.3)	5.4 (4.4-5.8)	4.7 (4.2-5.7)	0.18
LDL -C (mmol/L)	3.7 (2.3-3.8)	3.2 (2.4-4.1)	3.3 (2.8-3.6)	2.8 (2.3-3.3)	0.12
HDL-C (mmol/L)	1.3[a] (1.1-1.6)	1.3[a] (1-1.6)	1.3[a] (1.2-1.5)	1.2[b] (0.9-1.4)	0.04
TG (mmol/L)	1.1[a] (0.9-1.4)	1.6 [a,b] (1.1-2.2)	1.5 [a,b] (1-1.9)	1.6[b] (1.1-2)	0.01
Apo AI (mmol/L)	1.4[a] (1.3-	1.5[a] (1.3-	1.5[a] (1.4-1.7)	1.3[b] (1.0-	0.01

	1.6)	1.7)		1.4)	
Apo B (mmol/L)	1.1 (0.9-1.2)	1 (0.8-1.3)	1.1 (0.9-1.2)	1 (0.9-1.2)	0.66
tCa (mmol/L)	2.4(2.3-2.5)	2.5 (2.4-2.5)	2.4 (2.3-2.5)	2.4 (2.3-2.5)	0.25
iCa (mmol/L)	1.1 (1.07-1.1)	1.1 (1.1-1.2)	1.1 (1.1-1.2)	1.1 (1-1.3)	0.59
P (mmol/L)	1.03 (0.9-1.1)	1.1 (0.9-1.1)	1.1 (0.9-1.1)	1.1 (0.8-1.1)	0.74
Mg (mmol/L)	0.8 (0.8-0.9)	0.8 (0.8-0.9)	0.8 (0.7-0.9)	0.8 (0.7-0.9)	0.16
iPTH (pg/mL)	23[a] (20.4-25.5)	23.6[a] (20.5-26.8)	38.1[b] (34.1-41.9)	45.8[b] (39.7-51.9)	0.01
25(OH)D(nmol/L)	51.4 (42.5-60.3)	44.6 (37.9-51.2)	49.7 (40.3-59.1)	53.3 (47.3-59.1)	0.36

Groups designated by the same letter (a, b, c) do not exhibit significant differences in the post-hoc testing. Abbreviations: BMI: Body mass index; WC: Waist circumference; SP: Systolic pressure; DP: Diastolic pressure; MAP: Mean arterial pressure; HOMA-IR: Homeostasis model assessment of insulin resistance; tChol: Total cholesterol; LDL-C: Low-density lipoprotein cholesterol; HDL-C: High-density lipoprotein cholesterol; TG: Triglycerides; Apo A-1: Apolipoprotein A-1; Apo B: Apolipoprotein B; tCa: Total serum calcium concentration; iCa: Ionized serum calcium concentration; P: Serum phosphorus concentration; Mg: Serum magnesium concentration; iPTH: Intact parathyroid hormone serum concentration; 25(OH)D: Serum 25-hydroxyvitamin D concentration.

Table 2. Renal function profile of patients

Variables	Stage 1 *n*=25	Stage 2 *n*=30	Stage 3a *n*=26	Stage 3b *n*=30	*p*
Cys C (mg/L)	0.8[a] (0.7-1)	1[a] (0.9-1.1)	1.3[b] (1.1-1.5)	1.8[c] (1.4-1.9)	0.01
Creatinine (µmol/L)	88[a] (55.7-90.5)	81[a,b] (70-104)	100[b] (87-118)	125[b,c] (109-155)	0.01
Urea (mmol/L)	5.2[a] (4.5-5.4)	5.1[a,b] (4.6-6.7)	6.7[b] (5.3-8.1)	8.8[c] (7.6-10.2)	0.01
Uric Acid (µmol/L)	347[a] (279-396)	337[a] (283-386)	370[a,b] (301-406)	423[b] (371-462)	0.01
ACR (mg/mmol)	0.7 (0.7-1.8)	1.75 (1.33-6.2)	1.1 (0.8-2.9)	3.2 (1-8.6)	0.12
AER (mg/24h)	9.3 (7.8-20)	13.9 (6-89)	6.9 (3.2-31)	16 (5-81)	0.18
mGFR (ml/min/1.73m^2)	96[a] (94-98.2)	77[b] (72-84)	52[c] (48-56)	38.5[d] (35-41.9)	0.01
ASS-GFR (ml/min/1.73m^2)	112.9[a] (110.3-120.2)	104.8[a] (90.9-119.9)	84.5[b] (79.3-99)	85.1[b] (80.5-95.5)	0.01
DEV ASS GFR (ml/min/1.73m^2)	17.9[a] (14.8-22.9)	29.3[b] (21-41.1)	32[b] (29.1-42.2)	49.6[c] (43-55.6)	0.01
DEV ASS GFR (%)	16[a]	26.7[b]	40[c]	56.7[d]	0.01

	(11-21)	(22.4-33.2)	(37-43)	(52-60)	
mERPF (ml/min/1.73m^2)	520[a] (510-534)	436[b] (351-490)	298.5[c] (255-313)	235[d] (217-260)	0.01
ASS-ERPF (ml/min/1.73m^2)	633[a] (627-665)	595[a] (530-665)	500[b] (476-568)	503[b] (482-552)	0.01
DEV ASS ERPF (ml/min/1.73m^2)	135[a] (30-146)	166[b] (129-193)	221[b] (173-276)	279[c] (225-325)	0.01
DEV ASS ERPF (%)	20[a] (10-23)	26[b] (22-31)	46[c] (36-51)	55[d] (46-59)	0.01

Groups denoted by the same letter (a, b, c, d) do not exhibit significant differences in the post-hoc testing. Abbreviations: Cys C: Cystatin C; AER: Albumin excretion rate; ACR: Albumin-to-creatinine ratio; mGFR: Measured glomerular filtration rate; ASS-GFR: Age- and sex-specific glomerular filtration rate; DEV ASS GFR: Deviation for age- and sex-specific glomerular filtration rate; mERPF: Measured effective renal plasma flow; ASS-ERPF: Age- and sex-specific effective renal plasma flow; DEV ASS ERPF: Deviation for age- and sex-specific effective renal plasma flow.

Table 3. Correlation between iPTH and variables (*n*=111)

Variable	r	*p*
Age (years)	0.42	< 0.01
WC (cm)	0.22	0.02
BMI (kg/m^2)	0.27	0.01
MAP (mm/Hg)	0.14	0.15
Apo B (mmol/L)	0.10	0.26
LDL -C (mmol/L)	-0.05	0.59
HOMA IR	0.15	0.10
iCa (mmol/L)	-0.04	0.65
P (mmol/L)	-0.04	0.41
25 (OH)D (nmol/L)	-0.19	0.04
Cys C (mg/L)	0.48	< 0.01
mGFR (ml/min/1.73m$^{2)}$	-0.66	< 0.01
ASS-GFR (ml/min/1.73m^2)	-0.43	< 0.01
DEV-ASS GFR (%)	0.51	< 0.01
mERPF (ml/min/1.73m^2)	-0.68	< 0.01
ASS-ERPF (ml/min/1.73m^2)	-0.43	< 0.01
DEV-ASS ERPF (%)	0.57	< 0.01

Abbreviations: WC: Waist circumference; BMI: Body mass index; MAP: Mean arterial pressure; HOMA-IR: Homeostasis model assessment of insulin resistance; LDL-C: Low-density lipoprotein cholesterol; Apo B: Apolipoprotein B; iCa: Ionized serum calcium concentration; 25(OH)D: Serum 25-hydroxyvitamin D concentration; mGFR: Measured glomerular filtration rate; ASS-GFR: Age- and sex-estimated glomerular filtration rate; DEV ASS GFR: Deviation for age- and sex-estimated glomerular filtration rate; mERPF: Measured effective renal plasma flow; ASS-ERPF:

Age- and sex-specific effective renal plasma flow; DEV ASS ERPF: Deviation for age- and sex-estimated effective renal plasma flow; r: Spearman correlation coefficient; P: Level of significance.

Table 4. Univariate linear regression analysis of iPTH serum concentration and renal clearance measurements (mGFR and mERPF) among groups

iPTH (pg/mL)					
stage 1 (mGFR ≥90 ml/min/1.73m^2 with kidney damage, *n*= 25)					
	Unstandardized Coefficients		95% CI		
mGFR (ml/min/1.73m^2)	B	S.E. _B	Lower Bound	Upper Bound	P
slope	-0.25	0.45	-1.18	0.69	0.594
intercept	46.59	43.77	-43.96	137.14	0.298
mERPF (ml/min/1.73m^2)	B	S.E. _B	Lower Bound	Upper Bound	P
slope	0.09	0.03	0.03	0.15	0.003
intercept	-26.41	15.12	-57.67	4.88	0.094
stage 2 (mGFR 60–89 ml/min/1.73m^{2}with kidney damage, N= 30)					
	Unstandardized Coefficients		95% CI		
mGFR (ml/min/1.73m^2)	B	S.E. _B	Lower Bound	Upper Bound	P
slope	0.12	0.19	-0.28	0.52	0.549
intercept	14.44	15.23	-16.76	45.64	0.351
mERPF (ml/min/1.73m^2)	B	S.E. _B	Lower Bound	Upper Bound	
slope	-0.01	0.02	-0.05	0.02	0.469
intercept	29.61	8.31	12.59	46.63	0.001
stage 3a (mGFR 45–59 ml/min/1.73m^2, N= 26)					
	Unstandardized		95% CI		

	Coefficients				
mGFR (ml/min/1.73m^2)	B	S.E. _B	Lower Bound	Upper Bound	P
slope	0.32	0.41	-0.53	1.18	0.441
intercept	21.15	21.68	-23.59	65.89	0.34
mERPF (ml/min/1.73m^2)	B	S.E. _B	Lower Bound	Upper Bound	P
slope	-0.01	0.04	-0.92	0.08	0.918
intercept	39.38	12.57	13.43	65.32	0.005
stage 3b (mGFR 30–44 ml/min/1.73m^2, N= 30)					
	Unstandardized Coefficients		95% CI		
mGFR (ml/min/1.73m^2)	B	S.E. _B	Lower Bound	Upper Bound	P
slope	-1.85	0.64	-3.16	-0.55	0.007
intercept	116.88	24.58	66.52	167.24	< 0.001
mERPF (ml/min/1.73m^2)	B	S.E. _B	Lower Bound	Upper Bound	P
slope	-0.22	0.06	-0.33	-0.11	0.001
intercept	97.95	13.62	70.1	125.84	< 0.001

Abbreviations: iPTH: Intact parathyroid hormone serum concentration (pg/mL); mGFR: Measured glomerular filtration rate (mL/min/1.73 m²); mERPF: Measured effective renal plasma flow (mL/min/1.73 m²); B: Unstandardized coefficient; S.E._B: Standard error of B; P: Level of significance; 95% CI: 95% confidence interval for the unstandardized coefficient.

Table 5. Linear regression models analyzing the relationship between iPTH and variables related to renal clearance

	iPTH (pg/mL)					
Variable	Standardized Coefficients		Unstandardized Coefficients			
GFR-model	β	S.E._ β	B	S.E. _B	P	T
Intercept			20.280	21.839	0.355	
CKD stage	0.922	0.354	12.115	4.645	0.01	0.04
Interaction (CKD stage x mGFR)	-0.297	0.106	-0.156	0.056	0.006	0.449
mGFR (ml/min/1.73m^2)	0.088	0.319	0.057	0.206	0.782	0.050
ERPF-model	β	S.E._ β	B	S.E. _B	P	T
Intercept			-0.481	13.865	0.972	
CKD stage	1.423	0.298	18.699	3.909	< 0.001	0.051
Interaction (CKD stage x mERPF)	-0.605	0.146	-0.041	0.010	< 0.001	0.212
mERPF (ml/min/1.73m^2)	0.441	0.236	0.052	0.028	0.065	0.081

Abbreviations: iPTH: Intact parathyroid hormone serum concentration (pg/mL); CKD stage: Chronic kidney disease stage; mGFR: Measured glomerular filtration rate (mL/min/1.73 m²); mERPF: Measured effective renal plasma flow (mL/min/1.73 m²); β: Standardized coefficient; S.E._β: Standard error of β; B: Unstandardized coefficient; S.E._B: Standard error of B; P: Level of significance; T: Tolerance.

Table 6. Multiple linear regression models analyzing the relationship between iPTH and predictor variables

Model 1 AIC=814.645	iPTH (pg/mL)						
	Standardized Coefficients		Unstandardized Coefficients				
Predictor Variable	β	S.E._ β	B	S.E. _B	t-score	P	T
intercept			76.374	16.264	4.696	< 0.001	
CKD stage	0.978	0.092	12.847	1.213	10.591	< 0.001	0.419
Interaction (CKD stage x mGFR)	-0.347	0.083	-0.182	0.043	-4.184	< 0.001	0.520
Age (years)	-0.157	0.074	-0.145	0.068	-2.127	< 0.001	0.659
BMI (kg/m^2)	0.202	0.063	0.698	0.217	3.218	< 0.001	0.907
iCa (mmol/L)	-0.228	0.062	-44.917	12.142	-3.699	< 0.001	0.945
25(OH)D (nmol/L)	-0.325	0.062	-0.244	0.046	-5.259	< 0.001	0.934
Model 2 N=111 AIC=807.216	iPTH (pg/mL)						
	Standardized Coefficients		Unstandardized Coefficients				
Predictor Variable	β	S.E._ β	B	S.E. _B	t-score	P	T
intercept			56.777	14.112	4.023	<	

						0.001	
CKD stage	1.007	0.088	13.232	1.154	11.466	< 0.001	0.433
Interaction (CKD stage x mERPF)	-0.398	0.078	-0.027	0.005	-5.091	< 0.001	0.546
Age (years)	-0.169	0.071	-0.156	0.066	-2.376	< 0.001	0.660
BMI (kg/m^2)	0.203	0.060	0.702	0.209	3.364	0.001	0.917
iCa (mmol/L)	-0.158	0.059	-31.242	11.697	-2.671	0.009	0.952
25(OH)D (nmol/L)	-0.323	0.059	-0.242	0.045	-5.432	< 0.001	0.946

Abbreviations: iPTH: Intact parathyroid hormone serum concentration (pg/mL); AIC: Akaike's information criterion; CKD stage: Chronic kidney disease stage; mGFR: Measured glomerular filtration rate (mL/min/1.73 m^2); mERPF: Measured effective renal plasma flow (mL/min/1.73 m^2); BMI: Body mass index; iCa: Ionized serum calcium concentration; 25(OH)D: Serum 25-hydroxyvitamin D concentration; β: Standardized coefficient; S.E._β: Standard error of β; B: Unstandardized coefficient; S.E._B: Standard error of B; P: Level of significance; T: Tolerance.

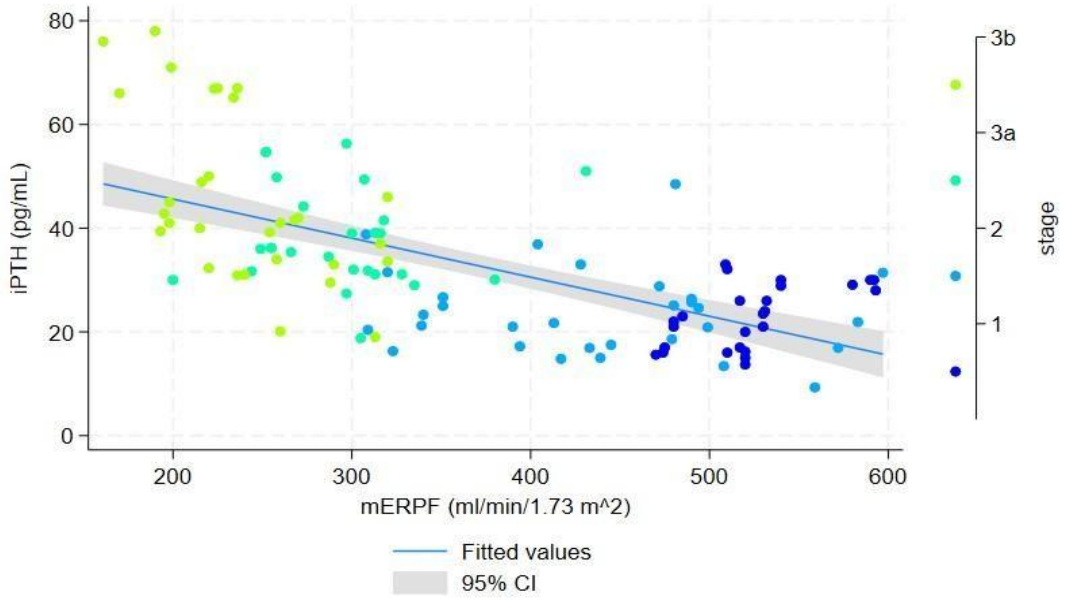

Figure 1. Scatter plot of serum iPTH versus mERPF in patients with early-stage CKD (*n* = 111). Each point represents an individual participant and is color-coded by chronic kidney disease stage (1–3b). The solid line shows the fitted values from a linear regression model (iPTH = 60.67 – 0.08 × mERPF), and the shaded area denotes the 95% confidence interval. Abbreviations: iPTH: Intact parathyroid hormone; mERPF: Measured effective renal plasma flow; CKD: Chronic kidney disease; CI: Confidence interval.

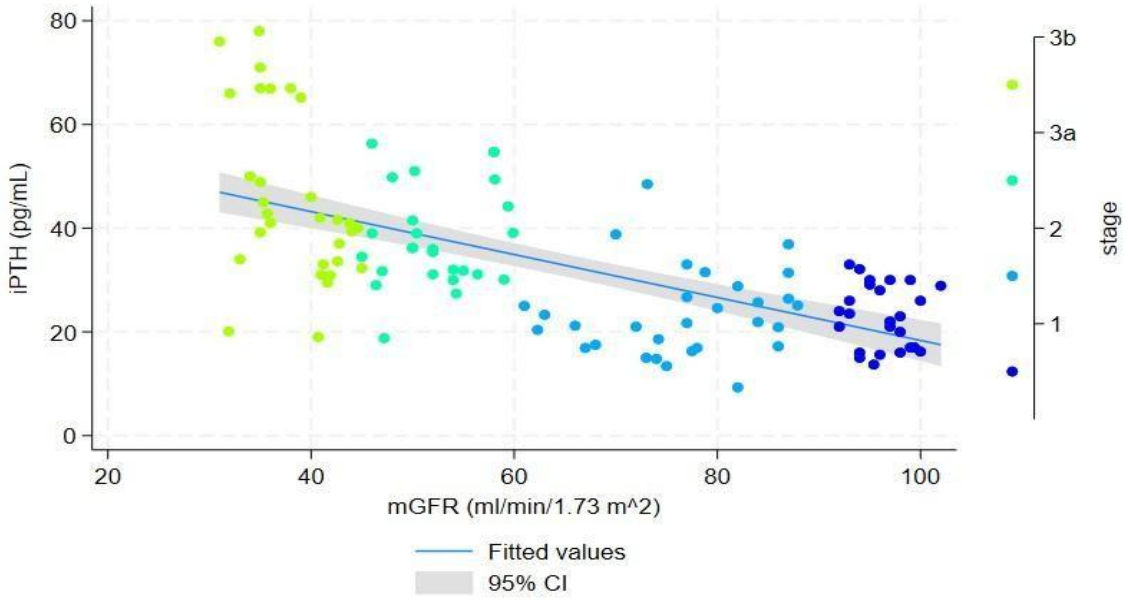

Figure 2. Scatter plot of serum iPTH versus mGFR in patients with early-stage CKD (*n* = 111). Each point represents an individual participant and is color-coded by CKD stage (1–3b). The solid line shows fitted values from a linear regression model (iPTH = 59.75 – 0.41 × mGFR), and the shaded area denotes the 95% CI. Abbreviations: iPTH: Intact parathyroid hormone; mGFR: Measured glomerular filtration rate; CKD: Chronic kidney disease; CI: Confidence interval.